Arch. Pharm. Res. (2013) 36:1178–1184
DOI 10.1007/s12272-013-0193-4

Archives of Pharmacal Research
www.springer.com/12272

REVIEW

Current status of PET-imaging probes of β-amyloid plaques

JaeHyung Koo · Youngjoo Byun

Received: 9 May 2013 / Accepted: 16 June 2013 / Published online: 1 July 2013

Abstract Alzheimer's disease (AD) is the most common form of dementia and is characterized by progressive cognitive decline and memory loss. One of pathological hallmarks of AD is the accumulation and deposition of β-amyloid (Aβ) plaques which is a potential target for the early diagnosis of AD. Positron emission tomography (PET), a sensitive radionuclide imaging technique, has provided opportunities to detect Aβ plaques of AD. PET-imaging probes of Aβ plaques have been extensively developed during the last decade. [^{18}F]Florbetapir, the ^{18}F-labeled PET-imaging probe of Aβ plaques, was recently approved by US Food and Drug Administration. A number of follow-on PET-imaging probes are currently being developed in academia and pharmaceutical companies. This article will discuss the recent development of PET-imaging probes from [^{11}C]PIB to [^{18}F]Florbetapir, which are in clinic trials, and several follow-on probes in preclinical stage.

Keywords Amyloid plaques · PET-imaging · Alzheimer's disease

Amyloid plaques and Alzheimer's disease (AD)

Alzheimer's disease (AD), described by Dr. Alois Alzheimer for the first time (Alzheimer 1907), is the most common form of dementia and is characterized by progressive cognitive decline and memory loss. As life expectancy has increased in developed and developing countries for the last decades, the number of elderly people is greatly on the rise. According to the World Health Organization (www.who.int), there were 18 million people living with AD worldwide in 2010, and this will increase to 34 million by 2025. As there are currently no therapeutic agents to cure or prevent AD, the early diagnosis of AD will provide an opportunity for AD patients to halt or slow down the progression of AD with medications on the market.

One of major pathological hallmarks of AD is the accumulation and deposition of β-amyloid (Aβ) plaques (Wong et al. 1985), leading to inflammation (Akiyama et al. 2000), oxidative stress (Galimberti and Scarpini 2011), and neurotoxicity in the brain (Broersen et al. 2010; Doi et al. 2009). Massive accumulation of Aβ has been observed in familial and sporadic AD patients. In particular, 42 amino acid long amyloid peptides ($A\beta_{42}$) are predominantly found in senile plaques of AD patients and are considered to play a critical role in the pathogenesis of AD (Citron et al. 1996). According to the amyloid hypothesis concerning the etiology of AD (Fig. 1), Aβ is generated from the amyloid precursor protein (APP) by the action of β-secretase and γ-secretase. The complex of Aβ with metal ions such as Cu^{2+} and Zn^{2+} leads to the aggregation of Aβ, which is the early event in the etiology of AD. Extracellular Aβ deposition leads to the activation of the downstream amyloid cascade pathway which is associated with the formation of neurofibrillary tangles (NFT) (Gomez-Isla et al. 1997). NFTs lead to the inflammation (Tuppo and Arias 2005), synapse loss (Gomez-Isla et al. 1996), neuronal dysfunction (SantaCruz et al. 2005), and, eventually, the death of susceptible neurons. Therefore, Aβ deposition

J. Koo (✉)
Department of Brain Science, Daegu Gyeongbuk Institute of Science & Technology (DGIST), 333, Tech Jungang Daero, Hyeonpung-Myeon, Dalseong-Gun, Daegu 711-873, South Korea
e-mail: jkoo001@dgist.ac.kr

Y. Byun (✉)
College of Pharmacy, Korea University, 2511 Sejong-ro, Sejong 339-700, South Korea
e-mail: yjbyun1@korea.ac.kr

Table 1 Physiochemical and biochemical properties of the β-amyloid imaging probes

Compound	K_i (nM)	Log *P*	MolLog *P*[a]	PSA[a] (Å^2)
^{11}C-PIB	0.87	1.30	3.74	38.26
^{18}F-GE-067	0.74	–	4.05	37.50
^{11}C-SB-13	3.18	3.20	3.94	28.00
^{18}F-AV-1	2.22	2.41	3.64	35.54
^{18}F-AV-45	2.87	1.70	2.80	43.83

[a] The theoretical values were calculated from Molsoft.com

is considered an attractive target for the diagnosis and treatment of AD.

Amyloid plaques and radionuclide-imaging

Although post-mortem pathological staining of brain tissue provides a definitive conclusion about the existence of Aβ plaques, there is currently no method to detect the accumulation level of Aβ plaques in living subjects. Modern radionuclide imaging techniques including positron emission tomography (PET), single photon emission computed tomography (SPECT), and magnetic resonance imaging (MRI) have provided opportunities to detect Aβ plaques from post-mortem histopathogical tissues and live human subjects. Among the imaging techniques, radionuclide-based imaging has become an important diagnostic tool of AD patients or people with mild cognitive impairment (MCI) due to the higher sensitivity and spatial resolution over the other imaging techniques. There are two major classes of Aβ-targeting radionuclide probes; one is PET probes labeled with ^{11}C and ^{18}F and the other is SPECT probes labeled with ^{123}I and ^{99m}Tc. Although SPECT-imaging is more cost-saving and convenient to prepare than PET-imaging, resolution of SPECT-imaging is not as good as PET-imaging and less translatable to the clinic. PET imaging of amyloid plaques is considered attractive in the discovery and development of diagnostic agents of AD because it can provide mapping of amyloid plaques in the brain of living subjects, which could predict the conversion from MCI to AD or from healthy subjects to MCI/AD patients. In addition, PET imaging can assist in monitoring the treatment efficacy of anti-AD therapeutic agents evaluated in clinic.

From [^{11}C]PIB to [^{18}F] AV-45 (Florbetapir)

The first successful PET-imaging probe of amyloid plaques in clinical studies is Pittsburg Compound B ([^{11}C]PIB in Fig. 2) labeled with [^{11}C]. It is a 6-hydroxybenzothiazole analog substituted with a 4-(methylamino)phenyl group at C-2. Clinical studies of [^{11}C]PIB with AD patients showed that it could detect the amyloid plaques in AD and identify people with MCI. This indicates that Aβ plaques are a potential biomarker for the diagnosis of AD and that Aβ-based PET imaging can predict the clinical outcome. Uptake and localization of [^{11}C]PIB in the brain region of AD patients were strongly correlated with post-mortem pathological results. Retention of [^{11}C]PIB in the frontal cortex was prominent in AD patients and it could distinguish AD patients from normal healthy subjects. However,

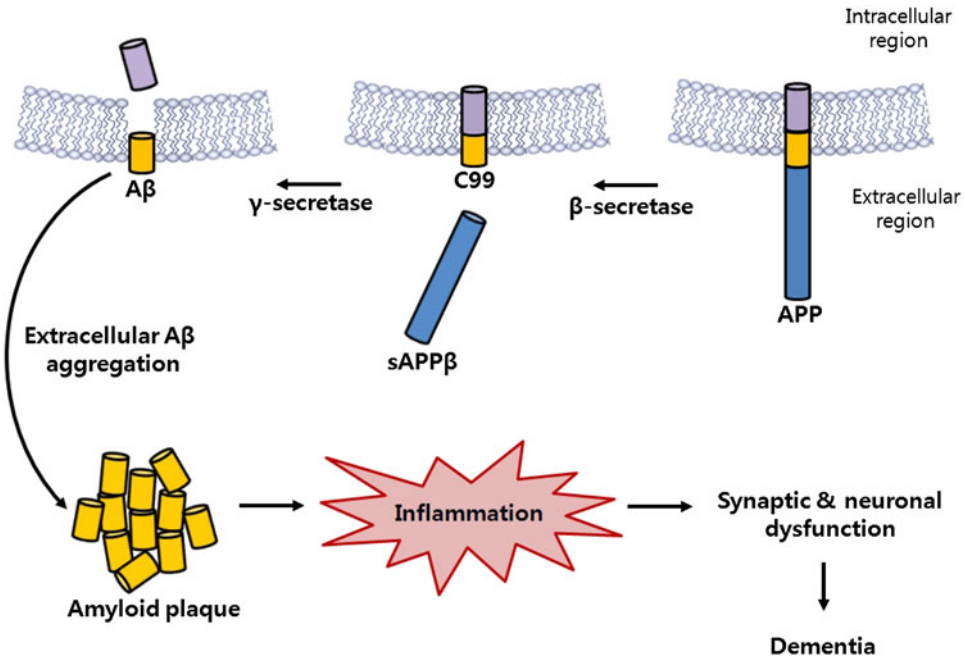

Fig. 1 Aβ deposition and amyloid cascade hypothesis. Amyloid precursor protein (APP) is an integral membrane protein. APP is cleaved into sAPPβ and the residual peptide (C99) by β-secretase and the subsequent action of γ-secretase. The cleaved Aβ is released into the extracellular region. Extracellular Aβ accumulation leads to the activation of the following sequential amyloid cascade: Aβ aggregates, amyloid plaque deposits, inflammation, synapse loss and neuronal dysfunction, and the death of susceptible neurons

the widespread clinical use of [^{11}C]PIB has the limitations of a short physical half-life of [^{11}C] and the requirement of a cyclotron facility on the clinical site. Therefore, [^{18}F]GE-067, the ^{18}F-labeled version of PIB, was developed in order to minimize the drawbacks of [^{11}C]PIB. [^{18}F] has a longer physical half-life (110 min) and better access to the clinical site by manufacturing and distribution compared to [^{11}C] (Koole et al. 2009). [^{18}F]Flutemetamol, the generic name of [^{18}F]GE-067 as shown in Fig. 2, exhibited brain uptake comparable to [^{11}C]PIB in phase II clinical studies (Vandenberghe et al. 2010).

Another class of Aβ imaging PET probes is stilbene-derived analogs. The initial lead compound of PET-imaging probes derived from stilbene is [^{11}C]SB-13 (4-*N*-methylamino-4′-hydroxy-stilbene). Although [^{11}C]SB-13 showed strong binding affinity for Aβ plaques with a K_i value of 3.1 nM, the short half-life of [^{11}C] and the undesirable physicochemical log *P* value hampered its translation into the clinic (Table 1). To overcome the physicochemical drawback of [^{11}C]SB-13, Kung and his co-workers introduced the polyethyleneglycol (PEG) group, which is known to increase water solubility, to lower the log *P* value, and to improve bioavailability of the parent compound. [^{18}F]AV-1, the SB-13 stilbene analog which contains a flexible fluoropegylated (FPEG) group instead of a hydroxyl group at the 4-position, provided better in vivo kinetic properties with comparable binding affinities (K_i = 2.2 nM) for Aβ plaques compared to [^{11}C]SB-13 (Zhang et al. 2005). Structure–activity relationship studies of PEG-substituted stilbene derivatives concluded that the mono- and di-methylation at the *N*-amino position of stilbene enhanced or maintained the binding affinities for Aβ plaques while the introduction of the free amino group dramatically abolished the binding affinities for Aβ (Zhang et al. 2005).

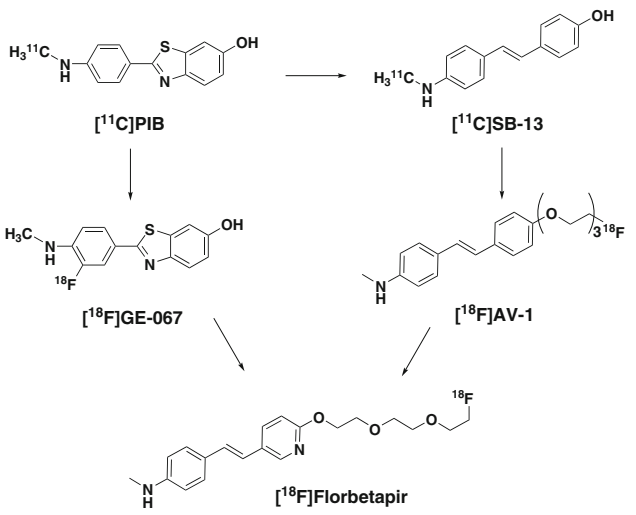

Fig. 2 Known PET imaging probes of amyloid plaques in the clinic

Further structural optimization of FPEG stilbene analogs resulted in the generation of a new potent class of styrylpyridine analogs by replacing the benzene ring of the stilbene analogs with pyridine. The FPEG styrylpyridine derivatives exhibited comparable binding affinities for amyloid plaques and better in vivo pharmacokinetic properties than the corresponding stilbene analogs (Zhang et al. 2007). One of them, termed ^{18}F-AV-45 (Fig. 2), was approved by the US Food and Drug Administration (FDA) in April 2012. The generic name of the first FDA-approved PET-imaging radiopharmaceutical of amyloid plaques is Florbetapir. Intravenous injection of Florbetapir showed excellent brain uptake at 2 min post injection and a rapid washout at 2 h with <1 % ID/g remaining in the brain. This kind of biochemical and physicochemical properties are extremely crucial for radionuclide-imaging probes. The dimethylated analog of Florbetapir also exhibited strong binding affinities for Aβ plaques and favorable physicochemical properties as compared to ^{18}F-Florbetapir. However, the demethylation process of the *N*,*N*-dimethylated moiety was so slow that the [^{18}F]-labeled dimethylated analog was retained in the region of interest as well as the whole body (Zhang et al. 2007).

^{18}F-Florbetapir: synthesis and biological evaluation

Radiosynthesis

Automated synthesis of [^{18}F]Florbetapir was reported by Kung and his co-workers (Liu et al. 2010). As shown in Scheme 1, the precursor **1** with the Boc group of the aniline moiety and tosylate group as a leaving group reacted with [^{18}F]KF/K222/K_2CO_3 in DMSO to afford **2** in 80 % radiochemical yield (RCY). Deprotection of the Boc group occurred by reacting **2** with 3.3 M HCl at 100 °C for 10 min. The purification of ^{18}F-Florbetapir was performed by solid phase extraction and did not require HPLC system, which saved the overall preparation time (Liu et al. 2010). According to Eli Lilly's recommendation guidelines, ^{18}F-Florbetapir with a radioactivity of 370 MBq (or 10 mCi) is administered via intravenous injection and its PET scanning is performed at 30–50 min post injection (Thompson 2012).

Biochemical properties

[^{18}F]Florbetapir has a high binding affinity for Aβ plaques with a K_i value of 2–3 nM (Herholz and Ebmeier 2011). The primary metabolite of [^{18}F]Florbetapir is the *N*-demethylated compound ([^{18}F]AV-45-M1 in Fig. 3) by the phase I metabolism reaction. The amine group was subsequently acetylated by the phase II conjugation reaction.

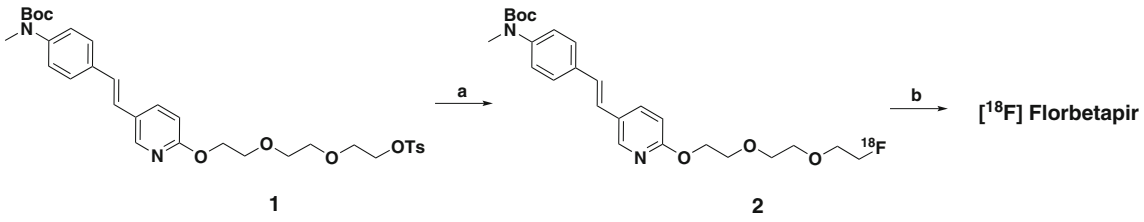

Scheme 1 Radiosynthesis of [^{18}F]Florbetapir

The terminal C–F bond was cleaved in rat microsomal enzyme systems in a non-clinical study and [^{18}F]AV-45-M3 was detected (Fig. 3; Yin et al. 2012).

Clinical studies

Initial human scanning studies of ^{18}F-Florbetapir showed a strong correlation with [^{11}C]PIB and provided comparable cutoff criteria to categorize human subjects as amyloid-positive or -negative (Wong et al. 2010). Another Aβ imaging study of the same individuals with [^{11}C]PIB and [^{18}F]Florbetapir at a 28-day interval distinguished the mild AD patient group from cognitively normal controls and exhibited strong correlation coefficients between [^{11}C]PIB and ^{18}F-Florbetapir (Wolk et al. 2012). Therefore, [^{11}C]PIB data obtained from clinical studies can be utilized to determine the regime of [^{18}F]Florbetapir. The other [^{18}F]Florbetapir-scanning during the clinical trial detected the Aβ plaques with a sensitivity of >90 % when compared with histopathology studies in 59 patients (Kingwell 2012).

According to a clinical study with cognitively normal patients, 70 % of Florbetapir-positive subjects progressed to MCI/AD over an average 4-year period while only 6 % of Florbetapir-negative did (Hauser et al. 2012). This result suggests that Florbetapir-positive healthy individuals may change their life styles to prevent or slow down the progression of AD. The quantitative assessment of Florbetapir-PET images of 46 subjects visually by two clinicians using the standard uptake value ratio in the regions of interest versus the reference region (cerebellum) exhibited high sensitivity and specificity (Camus et al. 2012). Perfusion imaging studies of [^{18}F]Florbetapir with 23 AD patients showed that Aβ plaque imaging with

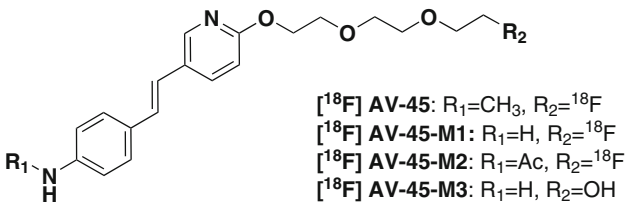

Fig. 3 [^{18}F]Florbetapir and its metabolites

[^{18}F]Florbetapir can detect the size and quantify Aβ plaques without spatial normalization provided by magnetic resonance (MR) (Hsiao et al. 2013). Based on a great number of positive results in clinical trials, [^{18}F]Florbetapir was approved by the US FDA on April 6, 2012, and is currently available for clinical use.

^{18}F-FDG PET has been utilized for detecting AD since 1980, because cerebral metabolic rate for glucose consumption in patients with AD showed a 20–30 % decrease compared with age-matched and healthy controls (Newberg et al. 2012). According to the recent studies of [^{18}F]Florbetapir with 19 AD patients or 21 normal controls, sensitivity and specificity of [^{18}F]Florbetapir were 95 and 95 %, respectively, while those of the [^{18}F]FDG-scans were 89 and 86 %, respectively (Newberg et al. 2012). According to [^{18}F]FDG-PET scan and [^{18}F]Florbetapir-PET scan studies with MCI subjects, Aβ deposition is more associated with cognitive decline in normal controls while glucose hypometabolism is more pronounced in late MCI and AD patients, indicating that Aβ deposition precedes metabolic changes (Landau et al. 2012). Aβ deposition is also more predominant in posterior and frontal regions of the brain while hypometabolism is in hippocampus (La Joie et al. 2012).

Recent extensive clinical studies of [^{18}F]Florbetapir with 555 individuals to assess brain Aβ levels at an early stage of AD indicated that the concentration of butyrylcholinesterase, one of therapeutic target proteins of AD, is strongly co-related with Aβ deposition (Ramanan et al. 2013).

Follow-on PET imaging probes of amyloid plaques

AZD 4694, an ^{18}F-labeled benzofuran analog developed by AstraZeneca, exhibited high affinity for Aβ plaques with a 2.3 nM K_i value in vitro (Fig. 4). According to a comparison experiment of AZD 4694 with Flutemetamol, AZD 4694 with a log D value of 2.8 showed lower non-specific binding than Flutametamol (log D = 3.2) in vitro and ex vivo (Jureus et al. 2010).

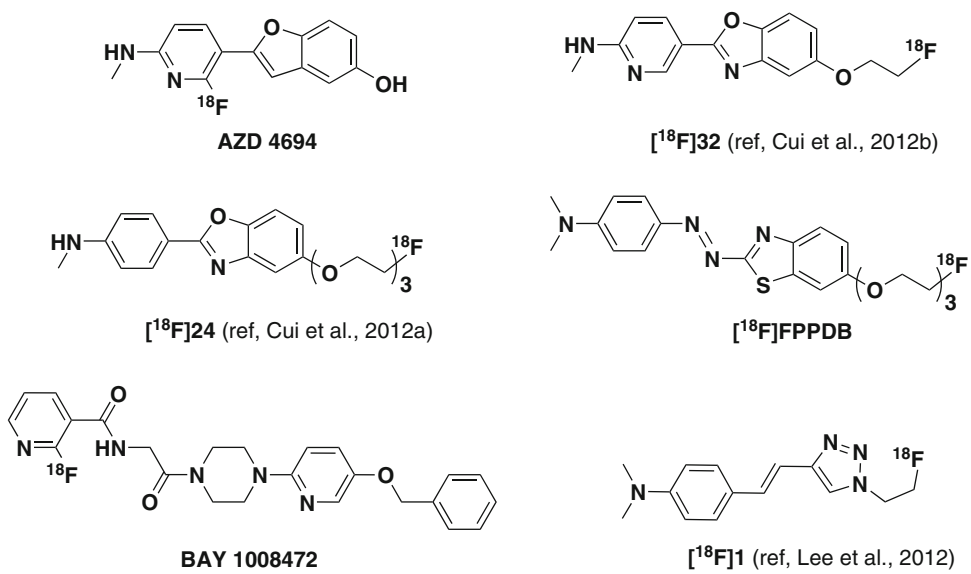

Fig. 4 Follow-on PET imaging probes of β-amyloid plaques

Recently, Lee et al. reported a styryltriazole-based ^{18}F-labeled PET probe, [^{18}F]**1** shown in Fig. 4. Brain uptake of [^{18}F]**1** in a normal mouse was 5.38 % ID at 2 min post injection with a wash-out of [^{18}F]**1** from brains of 0.52 % ID at 60 min post injection. The in vitro binding affinity of [^{18}F]**1** to Aβ was 12.8 nM (Lee et al. 2012).

[^{18}F]FPPDB, a phenyldiazenyl benzothiazole analog, showed high affinity for tau protein (K_i = 13 nM) as well as for Aβ plaques (K_i = 20 nM). NFTs are composed of phosphorylated tau protein which is another hallmark of AD. [^{18}F]FPPDB exhibited high brain uptake (4.28 % ID/g at 2 min post injection) and moderate washout (2.53 % ID/g at 60 min post injection) in a normal mouse (Matsumura et al. 2012).

[^{18}F]-labeled benzoxazole ligand, called [^{18}F]**24** as shown in Fig. 4, displayed high binding affinity for $A\beta_{1-42}$ aggregates (K_i = 9.3 nM). The log D value of [^{18}F]**24** is 3.09 which is in the range of good BBB penetration. Brain uptake of [^{18}F]**24** was observed with 8.12 % ID/g at 2 min and 3.04 % ID/g at 60 min after iv injection into normal ddY mouse (Cui et al. 2012a). *Ex vivo* autoradiography experiments of [^{18}F]**24** with post-mortem AD brain samples and Tg2576 mice demonstrated low non-specific binding in white matter area (Cui et al. 2012a).

[^{18}F]**32**, a FPEG pyridinylbenzoxazole derivative, showed the high in vitro binding affinity for $A\beta_{1-42}$ aggregates (K_i = 8.0 nM). Also, the $brain_{2min}/brain_{60min}$ ratio was 4.66, which is comparable to the probes in clinical trials and is suitable for amyloid PET imaging (Cui et al. 2012b). The log D value of [^{18}F]**32** was 3.52 while that of the corresponding tracer with a longer FPEG group was 2.86. However, [^{18}F]**32** with a short FPEG chain showed the higher brain uptake (7.23 % ID/g at 2 min) than the tracer with a longer FPEG group (4.05 % ID/g at 2 min), indicating that a short FPEG chain has better biochemical and pharmacokinetic properties than a long FPEG chain among a series of 2-pyridylbenzoxazole analogs.

BAY1008472, the *N*-4-benzyloxypyridyl piperazine analog labeled with ^{18}F, was optimized and developed from initial hits from a high-throughput screening of a large chemical library with synthetic $A\beta_{1-42}$ fibrils (Brockschnieder et al. 2012). It showed moderate in vitro binding affinity (IC_{50} = 39 nM) for amyloid plaques and excellent in vivo pharmacokinetic properties (6.45 % ID/g at 2 min and 0.70 % ID/g at 30 min post injection) (Brockschnieder et al. 2012).

Antibody-based PET probes labeled with [^{64}Cu] have been developed and evaluated in preclinical studies. The radio-labeled antibodies could cross the blood–brain barrier to sufficiently differentiate transgenic AD mice from wild type mice (McLean et al. 2013).

Perspectives

^{18}F-Florbetapir, the first FDA-approved PET tracer, is expected to be utilized widely at clinical sites. However, this new imaging agent may not replace post-mortem histopathology studies since Aβ imaging is not sufficient for the diagnosis of AD. Although imaging of Aβ plaques with [^{18}F]Florbetapir has limitations in detecting the earliest stages of Aβ deposition and some rare genetic variants, it has the potential to evaluate the efficacy of new AD therapeutic agents as well as to classify the AD patients entering into clinical trials.(Herholz 2012) Non-invasive PET imaging of Aβ plaques will be extended to monitor the earliest onset of AD in the brains of normal elderly healthy subjects and to evaluate the change of Aβ plaques

before clinical symptoms of AD begins. As PET-imaging tracers of Aβ plaques become widespread at clinical sites, appropriate criteria and guideline for brain Aβ imaging should be documented and provided for health professionals.

Acknowledgments This work was supported by the National Research Foundation of Korea (NRF) grant funded by the Korea Government (MEST) (No. 2012R1A1A1010000) and convergence science center (13-BD-0403). The authors thank Dr. Cockerham for critical reading and valuable comments and Mr. Kiwon Ok for editing the manuscript.

References

Akiyama, H., S. Barger, S. Barnum, B. Bradt, J. Bauer, G.M. Cole, N.R. Cooper, P. Eikelenboom, M. Emmerling, B.L. Fiebich, C.E. Finch, S. Frautschy, W.S.T. Griffin, H. Hampel, M. Hull, G. Landreth, L.F. Lue, R. Mrak, I.R. Mackenzie, P.L. Mcgeer, M.K. O'banion, J. Pachter, G. Pasinetti, C. Plata-Salaman, J. Rogers, R. Rydel, Y. Shen, W. Streit, R. Strohmeyer, I. Tooyoma, F.L. Van Muiswinkel, R. Veerhuis, D. Walker, S. Webster, B. Wegrzyniak, G. Wenk, T. Wyss-Coray, and N.W. Grp. 2000. Inflammation and Alzheimer's disease. *Neurobiology of Aging* 21: 383–421.

Alzheimer, A. 1907. Uber eine eigenartige Erkrankung der Hirnrinde. *Allgemeine Zeitschrift fur Psychiatrie und Psychisch-gerichtliche Medizin* 64: 146–148.

Brockschnieder, D., H. Schmitt-Willich, T. Heinrich, A. Varrone, B. Gulyas, M. Toth, J. Andersson, U. Boemer, S. Krause, M. Friebe, L. Dinkelborg, C. Halldin, and T. Dyrks. 2012. Preclinical characterization of a novel class of F-18-labeled PET tracers for amyloid-beta. *Journal of Nuclear Medicine* 53: 1794–1801.

Broersen, K., F. Rousseau, and J. Schymkowitz. 2010. The culprit behind amyloid beta peptide related neurotoxicity in Alzheimer's disease: oligomer size or conformation? *Alzheimers Research and Therapy* 2: 12.

Camus, V., P. Payoux, L. Barre, B. Desgranges, T. Voisin, C. Tauber, R. La Joie, M. Tafani, C. Hommet, G. Chetelat, K. Mondon, V. De La Sayette, J.P. Cottier, E. Beaufils, M.J. Ribeiro, V. Gissot, E. Vierron, J. Vercouillie, B. Vellas, F. Eustache, and D. Guilloteau. 2012. Using PET with 18F-AV-45 (florbetapir) to quantify brain amyloid load in a clinical environment. *European Journal of Nuclear Medicine and Molecular Imaging* 39: 621–631.

Citron, M., T.S. Diehl, G. Gordon, A.L. Biere, P. Seubert, and D.J. Selkoe. 1996. Evidence that the 42- and 40-amino acid forms of amyloid beta protein are generated from the beta-amyloid precursor protein by different protease activities. *Proceedings of the National Academy of Sciences USA* 93: 13170–13175.

Cui, M.C., M. Ono, H. Kimura, M. Ueda, Y. Nakamoto, K. Togashi, Y. Okamoto, M. Ihara, R. Takahashi, B.L. Liu, and H. Saji. 2012a. Novel F-18-labeled benzoxazole derivatives as potential positron emission tomography probes for imaging of cerebral beta-amyloid plaques in Alzheimer's disease. *Journal of Medicinal Chemistry* 55: 9136–9145.

Cui, M.C., X.D. Wang, P.R. Yu, J.M. Zhang, Z.J. Li, X.J. Zhang, Y.P. Yang, M. Ono, H.M. Jia, H. Saji, and B.L. Liu. 2012b. Synthesis and evaluation of novel F-18 labeled 2-pyridinylbenzoxazole and 2-pyridinylbenzothiazole derivatives as ligands for positron emission tomography (pet) imaging of beta-amyloid plaques. *Journal of Medicinal Chemistry* 55: 9283–9296.

Doi, Y., T. Mizuno, Y. Maki, S. Jin, H. Mizoguchi, M. Ikeyama, M. Doi, M. Michikawa, H. Takeuchi, and A. Suzumura. 2009. Microglia activated with the toll-like receptor 9 ligand CpG attenuate oligomeric amyloid beta neurotoxicity in in vitro and in vivo models of Alzheimer's disease. *American Journal of Pathology* 175: 2121–2132.

Galimberti, D., and E. Scarpini. 2011. Inflammation and oxidative damage in Alzheimer's disease: friend or foe? *Frontiers in Bioscience (Scholar Edition)* 3: 252–266.

Gomez-Isla, T., R. Hollister, H. West, S. Mui, J.H. Growdon, R.C. Petersen, J.E. Parisi, and B.T. Hyman. 1997. Neuronal loss correlates with but exceeds neurofibrillary tangles in Alzheimer's disease. *Annals of Neurology* 41: 17–24.

Gomez-Isla, T., J.L. Price, D.W. Mckeel, J.C. Morris, J.H. Growdon, and B.T. Hyman. 1996. Profound loss of layer II entorhinal cortex neurons occurs in very mild Alzheimer's disease. *Journal of Neuroscience* 16: 4491–4500.

Hauser, S.L., S.A. Josephson, and S.C. Johnston. 2012. Florbetapir: knowing one's future. *Annals of Neurology* 71: A6.

Herholz, K. 2012. Imaging cerebral amyloid plaques: clinical perspective. *Lancet Neurology* 11: 652–653.

Herholz, K., and K. Ebmeier. 2011. Clinical amyloid imaging in Alzheimer's disease. *Lancet Neurology* 10: 667–670.

Hsiao, I.T., C.C. Huang, C.J. Hsieh, S.P. Wey, M.P. Kung, T.C. Yen, and K.J. Lin. 2013. Perfusion-like template and standardized normalization-based brain image analysis using (18)F-florbetapir (AV-45/Amyvid) PET. *European Journal of Nuclear Medicine and Molecular Imaging* 40: 908–920.

Jureus, A., B.M. Swahn, J. Sandell, F. Jeppsson, A.E. Johnson, P. Johnstrom, J.A.M. Neelissen, D. Sunnemark, L. Farde, and S.P.S. Svensson. 2010. Characterization of AZD4694, a novel fluorinated A beta plaque neuroimaging PET radioligand. *Journal of Neurochemistry* 114: 784–794.

Kingwell, K. 2012. Alzheimer disease: Florbetapir-a useful tool to image amyloid load and predict cognitive decline in Alzheimer disease. *Nature Review Neurology* 8: 471.

Koole, M., D.M. Lewis, C. Buckley, N. Nelissen, M. Vandenbulcke, D.J. Brooks, R. Vandenberghe, and K. Van Laere. 2009. Whole-body biodistribution and radiation dosimetry of F-18-GE067: A radioligand for in vivo brain amyloid imaging. *Journal of Nuclear Medicine* 50: 818–822.

La Joie, R., A. Perrotin, L. Barre, C. Hommet, F. Mezenge, M. Ibazizene, V. Camus, A. Abbas, B. Landeau, D. Guilloteau, V. De La Sayette, F. Eustache, B. Desgranges, and G. Chetelat. 2012. Region-specific hierarchy between atrophy, hypometabolism, and beta-amyloid (Abeta) load in Alzheimer's disease dementia. *Journal of Neuroscience* 32: 16265–16273.

Landau, S.M., M.A. Mintun, A.D. Joshi, R.A. Koeppe, R.C. Petersen, P.S. Aisen, M.W. Weiner, and W.J. Jagust. 2012. Amyloid deposition, hypometabolism, and longitudinal cognitive decline. *Annals of Neurology* 72: 578–586.

Lee, I., Y.S. Choe, J.Y. Choi, K.H. Lee, and B.T. Kim. 2012. Synthesis and evaluation of F-18-labeled styryltriazole and resveratrol derivatives for beta-amyloid plaque imaging. *Journal of Medicinal Chemistry* 55: 883–892.

Liu, Y., L. Zhu, K. Plossl, S.R. Choi, H. Qiao, X. Sun, S. Li, Z. Zha, and H.F. Kung. 2010. Optimization of automated radiosynthesis of [18F]AV-45: a new PET imaging agent for Alzheimer's disease. *Nuclear Medicine and Biology* 37: 917–925.

Matsumura, K., M. Ono, H. Kimura, M. Ueda, Y. Nakamoto, K. Togashi, Y. Okamoto, M. Ihara, R. Takahashi, and H. Saji. 2012. F-18-labeled phenyldiazenyl benzothiazole for in vivo imaging of neurofibrillary tangles in Alzheimer's disease brains. *ACS Medicinal Chemistry Letters* 3: 58–62.

McLean, D., M.J. Cooke, R. Albay 3rd, C. Glabe, and M.S. Shoichet. 2013. Positron emission tomography imaging of fibrillar

parenchymal and vascular amyloid-beta in TgCRND8 mice. *ACS Chemical Neuroscience* 4: 613–623.

Newberg, A.B., S.E. Arnold, N. Wintering, B.W. Rovner, and A. Alavi. 2012. Initial clinical comparison of 18F-florbetapir and 18F-FDG PET in patients with Alzheimer disease and controls. *Journal of Nuclear Medicine* 53: 902–907.

Ramanan, V.K., S.L. Risacher, K. Nho, S. Kim, S. Swaminathan, L. Shen, T.M. Foroud, H. Hakonarson, M.J. Huentelman, P.S. Aisen, R.C. Petersen, R.C. Green, C.R. Jack, R.A. Koeppe, W.J. Jagust, M.W. Weiner, and A.J. Saykin. 2013. APOE and BCHE as modulators of cerebral amyloid deposition: a florbetapir PET genome-wide association study. *Molecular Psychiatry*. doi: 10.1038/mp.2013.19.

SantaCruz, K., J. Lewis, T. Spires, J. Paulson, L. Kotilinek, M. Ingelsson, A. Guimaraes, M. Deture, M. Ramsden, E. Mcgowan, C. Forster, M. Yue, J. Orne, C. Janus, A. Mariash, M. Kuskowski, B. Hyman, M. Hutton, and K.H. Ashe. 2005. Tau suppression in a neurodegenerative mouse model improves memory function. *Science* 309: 476–481.

Thompson, C.A. 2012. Radioactive agent approved as part of Alzheimer disease workup. *American Journal of Health System Pharmacy* 69: 818.

Tuppo, E.E., and H.R. Arias. 2005. The role of inflammation in Alzheimer's disease. *International Journal of Biochemistry and Cell Biology* 37: 289–305.

Vandenberghe, R., K. Van Laere, A. Ivanoiu, E. Salmon, C. Bastin, E. Triau, S. Hasselbalch, I. Law, A. Andersen, A. Korner, L. Minthon, G. Garraux, N. Nelissen, G. Bormans, C. Buckley, R. Owenius, L. Thurfjell, G. Farrar, and D.J. Brooks. 2010. F-18-flutemetamol amyloid imaging in Alzheimer disease and mild cognitive impairment a phase 2 trial. *Annals of Neurology* 68: 319–329.

Wolk, D.A., Z. Zhang, S. Boudhar, C.M. Clark, M.J. Pontecorvo, and S.E. Arnold. 2012. Amyloid imaging in Alzheimer's disease: comparison of florbetapir and Pittsburgh compound-B positron emission tomography. *Journal of Neurology, Neurosurgery and Psychiatry* 83: 923–926.

Wong, C.W., V. Quaranta, and G.G. Glenner. 1985. Neuritic plaques and cerebrovascular amyloid in Alzheimer-disease are antigenically related. *Proceedings of the National Academy of Sciences USA* 82: 8729–8732.

Wong, D.F., P.B. Rosenberg, Y. Zhou, A. Kumar, V. Raymont, H.T. Ravert, R.F. Dannals, A. Nandi, J.R. Brasic, W.G. Ye, J. Hilton, C. Lyketsos, H.F. Kung, A.D. Joshi, D.M. Skovronsky, and M.J. Pontecorvo. 2010. In vivo imaging of amyloid deposition in Alzheimer disease using the radioligand F-18-AV-45 (flobetapir F 18). *Journal of Nuclear Medicine* 51: 913–920.

Yin, W., X. Zhou, J.P. Qiao, and L. Zhu. 2012. Study the pharmacokinetics of AV-45 in rat plasma and metabolism in liver microsomes by ultra-performance liquid chromatography with mass spectrometry. *Biomedical Chromatography* 26: 666–671.

Zhang, W., M.P. Kung, S. Oya, C. Hou, and H.F. Kung. 2007. F-18-labeled styrylpyridines as PET agents for amyloid plaque imaging. *Nuclear Medicine and Biology* 34: 89–97.

Zhang, W., S. Oya, M.P. Kung, C. Hou, D.L. Maier, and H.F. Kung. 2005. F-18 polyethyleneglycol stilbenes as PET imaging agents targeting A beta aggregates in the brain. *Nuclear Medicine and Biology* 32: 799–809.